PHYSICAL REVIEW D VOLUME 26, NUMBER 7 1 OCTOBER 1982

Quantum-chromodynamic corrections to deep-inelastic Compton scattering

D. W. Duke and J. F. Owens
Physics Department, Florida State University, Tallahassee, Florida 32306
(Received 19 April 1982)

Deep-inelastic Compton scattering is a potentially useful source of information concerning the short-distance structure of hadrons. We present here results for several types of corrections to the basic Compton subprocess. Contributions from subprocesses involving photon distribution and fragmentation functions are shown to be small in the high-p_T region in the leading-logarithm approximation. The next-to-leading-order corrections from the subprocesses $\gamma q \to \gamma q g$ and $\gamma g \to \gamma q \bar{q}$ are also calculated and found to be small over a wide rapidity range for large p_T values. These small corrections suggest that the deep-inelastic Compton process will indeed be a useful reaction to measure.

I. INTRODUCTION

The study of hadronic scattering processes with large transverse momenta is a potentially rich source of information pertaining to the short-distance structure of hadrons. However, such reactions receive contributions from many different types of parton subprocesses and the resulting complicated superposition makes it difficult to draw unambiguous conclusions from the data. The situation is improved somewhat if one allows photons as well as hadrons to take part in the high-p_T reactions. For both high-p_T photoproduction and the high-p_T production of direct photons a reduction in the number of parton subprocesses occurs at each order of perturbation theory as compared to the purely hadronic case. Furthermore, since the photon couples to the quark charge the relative weighting of the various subprocesses is different than in the purely hadronic case. Also, since the photon can participate directly in the relevant subprocess, closer contact is made with the underlying parton kinematics. Following the above line of reasoning one might conclude that if one photon is good then two are better. This leads inevitably to the study of deep-inelastic (DI) Compton scattering, $\gamma p \to \gamma + X$.

It was suggested a long time ago that the experimental study of DI Compton scattering would provide an interesting and important test of the parton model of deep-inelastic processes.[1] In particular, assuming that the fundamental parton subprocess is just γ-quark elastic scattering, one can measure the ratio of the average fourth power of the quark charges to the average second power of the quark charges. Such a measurement would be an important test of the fractionally charged quark model.

Since the original parton-model investigation of deep-inelastic Compton scattering, it has become clear that quantum chromodynamics (QCD) is an excellent candidate theory of strong interactions. In particular, the asymptotic freedom of QCD allows a systematic perturbative investigation of all deeply inelastic scattering processes. The great breadth of application of perturbative QCD follows from the factorization theorem, which provides a fundamental justification of the application of parton-model ideas.[2] In this paper we will apply these properties of perturbative QCD to investigate in some depth the relationship between DI Compton and lepton scattering. In particular we will estimate to what extent the ratio $\langle e^4 \rangle / \langle e^2 \rangle$ is affected by various QCD-induced modifications to the original parton-model cross section for DI Compton scattering.

These QCD-induced modifications are of essentially two types. First, we have additional contributions to the basic $\gamma + q \to \gamma + q$ subprocess even at the leading-logarithm level. These new contributions are consequences of the anomalous, or pointlike part of the photon structure function.[3] These contributions have been investigated previously and are reviewed in Sec. II of this paper.[4] Second, we have the higher-order strong-interaction corrections beyond the leading-logarithm level.

Our calculation is a rather interesting example of a higher-order QCD calculation for several reasons. First, it is sufficiently simple that one can include all the allowed order-$\alpha^2 \alpha_s$ subprocesses,

i.e., $\gamma+q\rightarrow\gamma+q+g$ and $\gamma+g\rightarrow\gamma+q+\bar{q}$. The corresponding calculation for purely hadronic high-p_T scattering is very complex because of the much larger number of subprocesses involved. Second, the interplay between the various types of corrections may be observed. This provides a potentially useful test of ideas for choosing the optimum factorization scale for deep-inelastic processes. Third, the calculation is a pedagogically interesting example of the QCD hard-scattering factorization theorem implemented beyond the leading-logarithm approximation.

The plan of the paper is as follows. In Sec. II the results of the leading-logarithm calculation are presented and discussed. In Sec. III the calculation of the order-$\alpha^2\alpha_s$ corrections is described and the results are compared to the lowest-order Compton process. Our conclusions are contained in Sec. IV and some technical details are presented in two Appendices.

II. LEADING-LOGARITHM CORRECTIONS

In this section we shall consider a variety of subprocesses which contribute to the production of high-p_T photons and, therefore, provide backgrounds to the Compton process. All of these subprocesses will eventually yield order-α^2 contributions at the leading-logarithm level, so a quantitative measurement of $\langle e^4\rangle/\langle e^2\rangle$, as explained in the Introduction, is only possible provided these backgrounds are small.

The approximation of colinear parton kinematics will be used. With only one initial-state hadron, parton-transverse-momentum smearing effects should not be as important as in purely hadronic scattering. If only two-body hard-scattering subprocesses are taken into account, the invariant cross section for high-p_T photon photoproduction can be written as

$$E\frac{d^3\sigma}{dp^3}(\gamma p\rightarrow\gamma+x)=\sum_{abc}\int dx_a\,dx_b\frac{dx_c}{x_c^2}G_{a/\gamma}(x_a,Q^2)G_{b/p}(x_b,Q^2)D_{\gamma/c}(x_c,Q^2)\frac{s}{\pi}\frac{d\sigma}{dt}(ab\rightarrow cd)\delta(s+t+u)\,, \tag{1}$$

where s, t, and u denote the parton variables for the hard-scattering subprocesses. The effects of higher-order terms are included, to leading-logarithmic accuracy, by using scale-violating distribution and fragmentation functions. The factorization scale for these functions, Q^2, will be discussed later.

There are four classes of subprocesses which must be included in Eq. (1):

(I) $a=c=\gamma$, $b=q$. This is just the order-α^2 Compton subprocess. To leading order in α we can take

$$G_{\gamma/\gamma}(x)=D_{\gamma/\gamma}(x)=\delta(1-x)$$

so that for this class there are no remaining integrations.

(II) $a=\gamma$, b and $c=q$ or g. This class included the order-$\alpha\alpha_s$ subprocesses $\gamma q\rightarrow gq$ and $\gamma g\rightarrow q\bar{q}$. The fragmentation functions $D_{\gamma/q}$ and $D_{\gamma/g}$ are of order α/α_s so that the net contribution is of order α^2.

(III) $c=\gamma$, a and $b=q$ or g. For this class the order-$\alpha\alpha_s$ subprocesses $qg\rightarrow\gamma q$ and $q\bar{q}\rightarrow\gamma g$ are convoluted with the order-α/α_s photon distribution functions $G_{q/\gamma}$ and $G_{g/\gamma}$.

(IV) a, b, and $c=q$ or g. Here both fragmentation and distribution functions are convoluted with

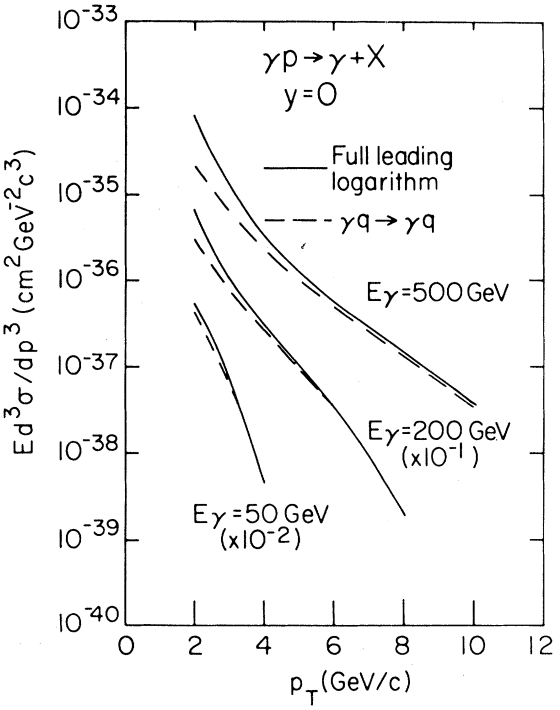

FIG. 1. Predictions from the full leading-logarithm calculation (solid curves) and the leading-logarithm Compton term alone (dashed curves) versus p_T at $y=0$ for several beam momenta. For clarity the curves have been multiplied by the factors in parentheses.

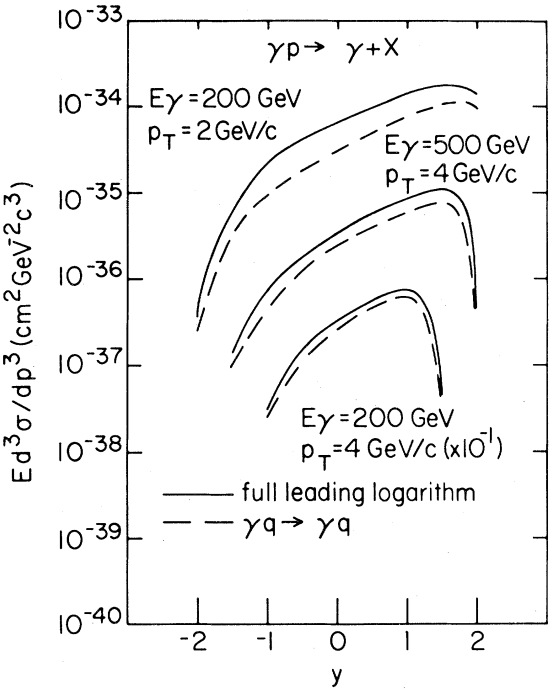

FIG. 2. Same as Fig. 1 but versus y at fixed p_T.

order-α_s^2 subprocesses to give an overall α^2 contribution.

The expressions for the relevant subprocesses are discussed in Appendix A. The photon distribution and fragmentation functions have been calculated in the leading-logarithm approximation.[3] Convenient parametrizations are also included in Appendix A. The nucleon distribution functions have been obtained by fitting deep-inelastic structure function data and will be discussed further in Sec. III. For the predictions to be discussed in this section we have used the one-loop expression for α_s:

$$\alpha_s(Q^2)=12\pi/[(33-2f)\ln(Q^2/\Lambda^2)]\ ,$$

with $\Lambda=380$ MeV/c, $f=4$, and Q^2 has been taken as $2p_T^2$.

In Fig. 1 the predictions of Eq. (1) for the invariant cross section are shown versus p_T at $y=0$ for a variety of beam energies. Here y is the photon rapidity in the overall center-of-mass system. The Compton contribution is shown separately by the dashed curves. It is clear that for large $x_T=2p_T/s$ the Compton subprocess is dominant.

In Fig. 2 the rapidity dependence at fixed p_T is illustrated. The ratio of the total to the Compton contribution is seen to vary rather slowly with rapidity and, as before, to decrease with increasing p_T.

In order to further illustrate this behavior, in

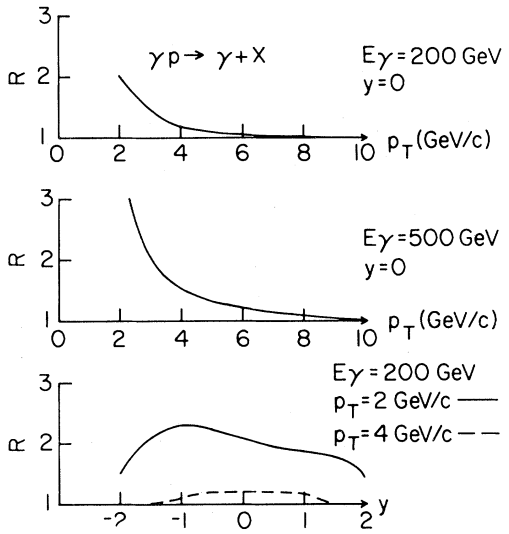

FIG. 3. The ratio R of the full leading-logarithm calculation to the leading-logarithm Compton term.

Fig. 3 several examples of the ratio of the full leading-logarithm result to the Compton contribution are shown. Once again it can be seen that the Compton subprocess dominates in the high-p_T region.

These results suggest that the contributions from various fragmentation-type subprocesses should not obscure the Compton subprocess provided that the transverse momentum is sufficiently large, say $x_T \geq 0.4$. This same conclusion was reached in

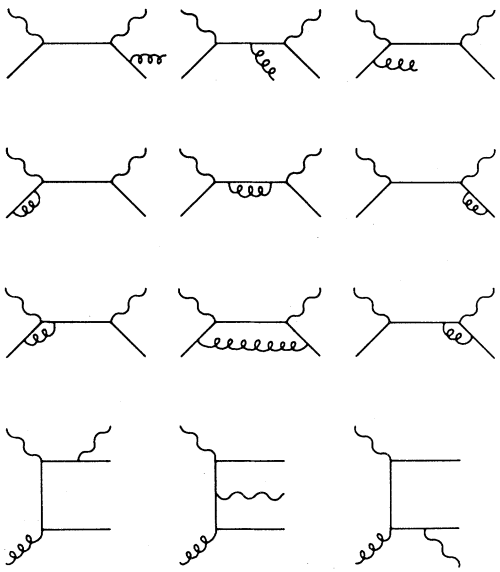

FIG. 4. Feynman graphs for the subprocesses $\gamma q \to \gamma q g$ and $\gamma g \to \gamma q \bar{q}$. The virtual graphs are shown as well. Additional graphs are obtained by $s \leftrightarrow u$ crossing.

Ref. 4 which also contains an interesting discussion of the different kinematics associated with the various contributions listed above.

III. NONLEADING CORRECTIONS

In this section the results of our calculation of the order-$\alpha^2\alpha_s$ corrections to the Compton subprocess will be presented. From the discussion in the preceding section it is clear that there are in fact four classes of higher-order corrections involving subprocesses of order $\alpha^2\alpha_s$, $\alpha\alpha_s^2$, and α_s^3 convoluted with the appropriate photon fragmentation and/or distribution functions. Inclusion of all of these terms goes well beyond the scope of this paper. Here we shall limit our consideration to the contribution of the $\gamma g \to \gamma q\bar{q}$ and $\gamma q \to \gamma qg$ subprocesses shown in Fig. 4. In the previous section it was shown that for large values of x_T the various contributions involving photon distribution or fragmentation functions were small. It therefore seems reasonable to neglect the higher-order corrections to these small terms. That leaves only those corrections where the photons take part directly in the subprocess. These terms should provide the largest nonleading corrections.

The actual calculation follows closely that of Ellis *et al.*,[5] except for our convention concerning the definition of the parton distributions. We have chosen to use universal, process independent, parton distributions and to include the next-to-leading-order corrections for a given process in the relevant hard-scattering cross-section expressions. The quark and gluon distributions have been determined in this way by fitting deep-inelastic data using the cross-section expressions calculated beyond the leading order. For the photon distribution and fragmentation functions this procedure is not necessary since there are no unknown functions to be determined. Furthermore, the next-to-leading-order contributions from processes involving the photon distribution and/or fragmentation functions have not been included, as discussed above.

In this section only the basic outline of the calculation will be discussed. An indication of the calculational details can be found in Appendix B.

The contributions of order α^2 and $\alpha^2\alpha_s$ to the deep-inelastic Compton cross section can be written as

$$E\frac{d^3\sigma}{dp^3}(\gamma p \to \gamma + X) = \int dx_b \left\{ \sum_{i=1}^{2f} G_{q_i/p}(x_b) \left[E\frac{d^3\sigma}{dp^3}(\gamma q_i \to \gamma q_i) + E\frac{d^3\sigma}{dp^3}(\gamma q_i \to \gamma q_i g) \right] + G_{g/p}(x_b) \sum_{j=1}^{f} \frac{Ed^3\sigma}{dp^3}(\gamma g \to \gamma q_j \bar{q}_j) \right\} . \tag{2}$$

In Eq. (2) the parton distribution functions do not yet contain any Q^2 dependence. Now, in each order of perturbation theory the leading term will be proportional to $(\alpha_s \ln Q^2/\Lambda^2)^m$ where Q^2 is the square of some typical large momentum transfer. These terms can be summed and their effects can be incorporated into scale-violating distribution and fragmentation functions giving a result of the form of Eq. (1). Now, however, we have additional nonleading contributions coming from the order-$\alpha^2\alpha_s$ terms in Eq. (2). If we retain only those terms which receive contributions from the order-$\alpha^2\alpha_s$ subprocesses listed above, then the invariant cross section can be written as

$$\begin{aligned} E\frac{d^3\sigma}{dp^3}(\gamma p \to \gamma + X) = {} & \int dx_b \sum_{i=1}^{2f} G_{q_i/p}(x_b,Q^2) \left[E\frac{d^3\sigma}{dp^3}(\gamma q_i \to \gamma q_i) + K_1 \right] \\ & + \int dx_b \frac{dx_c}{x_c^2} \left[\sum_{j=1}^{f} G_{g/p}(x_b,Q^2) E\frac{d^3\sigma}{dp^3}(\gamma g \to q_j\bar{q}_j)[D_{\gamma/q_j}(x_c,Q^2) + D_{\gamma/\bar{q}_j}(x_c,Q^2)] \right. \\ & \left. + \sum_{i=1}^{2f} G_{q_i/p}(x_b,Q^2) E\frac{d^3\sigma}{dp^3}(\gamma_{q_i} \to q_i g) D_{\gamma/q_i}(x_c,Q^2) \right] \\ & + \int dx_a\, dx_b \sum_{i=1}^{2f} G_{q_i/\gamma}(x_a,Q^2) \left[G_{g/p}(x_b,Q^2) E\frac{d^3\sigma}{dp^3}(q_i g \to \gamma q_i) \right. \\ & \left. + G_{\bar{q}_i/p}(x_b,Q^2) E\frac{d^3\sigma}{dp^3}(q_i\bar{q}_i \to \gamma g) \right] \\ & + \int dx_b G_{g/p}(x_b,Q^2) K_2 . \end{aligned} \tag{3}$$

In Eq. (3) the terms K_1 and K_2 are the finite, order-$\alpha^2\alpha_s$ corrections terms that we will calculate. The only terms that could formally be present in Eq. (3) but which are not included are the class IV leading-logarithm terms involving purely hadronic subprocesses as well as the order-$\alpha\alpha_s{}^2$ and order-$\alpha_s{}^3$ corrections. Since we know that the class II–IV terms are already small in the region of interest ($x_T \geq 0.4$), this is an acceptable approximation. The important point to decide is the size of K_1 and K_2. Next, to order α_s, one can write the required Q^2-dependent distribution and fragmentation functions as follows:

$$
\begin{aligned}
G_{q_i/p}(x,Q^2) &= G_{q_i/p}(x) + \frac{\alpha_s}{2\pi}\tilde{t}\int_x^1 \frac{dy}{y}\left[P_{qq}\left[\frac{x}{y}\right]G_{q_i/p}(y) + P_{qg}\left[\frac{x}{y}\right]G_{g/p}(y)\right], \\
G_{g/p}(x,Q^2) &= G_{g}/p(x) + \frac{\alpha_s}{2\pi}\tilde{t}\int_x^1 \frac{dy}{y}\left[\sum_{j=1}^{2f} P_{gq}\left[\frac{x}{y}\right]G_{q_i/p}(y) + P_{gg}\left[\frac{x}{y}\right]G_{g/p}(y)\right], \\
G_{q_i/\gamma}(x,Q^2) &= \frac{\alpha}{2\pi}e_i{}^2 P_{q\gamma}(x)\tilde{t}, \\
D_{\gamma/q_i}(x,Q^2) &= \frac{\alpha}{2\pi}e_i{}^2 P_{\gamma q}(x)\tilde{t},
\end{aligned}
\tag{4}
$$

where $\tilde{t}=\ln Q^2/\mu^2$ and μ^2 is the renormalization point. The next step is to substitute Eqs. (4) into Eq. (3), retaining only order-α^2 and $-\alpha^2\alpha_s$ terms. The result is then set equal to Eq. (2), thereby allowing one to obtain expressions for the finite corrections terms K_1 and K_2. The result for K_1 is

$$
\begin{aligned}
\int dx_b \sum_i G_{q_i/p}(x_b)K_1 = \int dx_b \Bigg[& \sum_i G_{q_i/p}(x_b) E\frac{d^3\sigma}{dp^3}(\gamma q_i \to \gamma q_i g) \\
& - \frac{\alpha_s}{2\pi}\tilde{t}\sum_i \int \frac{dy}{y} P_{qq}\left[\frac{x_b}{y}\right] G_{q_i/p}(y) E\frac{d^3\sigma}{dp^3}(\gamma q_i \to \gamma q_i) \\
& - \frac{\alpha}{2\pi}\sum_i e_i{}^2\tilde{t}\int dx_a G_{q_i/p}(x_b) P_{q\gamma}(x_a) E\frac{d^3\sigma}{dp^3}(\bar{q}_i q_i \to \gamma g) \\
& - \frac{\alpha}{2\pi}\sum_i e_i{}^2\tilde{t}\int \frac{dx_c}{x_c{}^2} G_{q_i/p}(x_b) P_{\gamma q}(x_c) E\frac{d^3\sigma}{dp^3}(\gamma q_i \to q_i g)\Bigg].
\end{aligned}
\tag{5}
$$

The expression for K_2 has a similar form. In both Eqs. (4) and (5) the function P_{ij} are the usual Altarelli-Parisi[6] functions. Note that $P_{q\gamma}=6P_{qg}$ and $P_{\gamma q}=3/4P_{gq}$.

The expression for K_1 can be further simiplified by noting that there is a δ function contained in the definition of the two-body invariant cross section. This allows the indicated integrations to be performed leaving a straightforward result for the two correction terms. For this purpose it turns out to be convenient to switch to a new set of kinematic variables defined by[5]

$$v = 1 + t/s, \quad w = -u/(s+t).$$

In terms of these variables the expression for K_1 can be written as follows:

$$
\begin{aligned}
\pi s K_1 = & \frac{1}{v}\frac{d\sigma}{dv\,dw}(\gamma q_i \to \gamma q_i g) \\
& - \frac{\tilde{t}}{2\pi}\left[\frac{\alpha_s}{1-vw}P_{qq}\left[\frac{1-v}{1-vw}\right]\frac{d\sigma}{dv}\left[s\frac{1-v}{1-vw}, t\right]_{\gamma q_i \to \gamma q_i} + e_i{}^2\frac{\alpha}{v}P_{q\gamma}(w)\frac{d\sigma}{dv}(sw, -sw(1-v))_{\bar{q}_i q_i \to \gamma g}\right. \\
& \left. + e_i{}^2\frac{\alpha}{(1-v+vw)}P_{\gamma q}(1-v+vw)\frac{d\sigma}{dv}\left[s, -\frac{s(1-v)}{1-v+w}\right]_{\gamma q_i \to q_i g}\right].
\end{aligned}
\tag{6}
$$

A similar expression can be written for K_2.

Now, the cross section for the $2\to 3$ subprocess in Eq. (6) contains mass singularities which must be regulated in some fashion. We have chosen to use dimensional regularization,[7] working in $n=4-2\epsilon$ dimensions.

In this case the mass singularities appear as terms proportional to $1/\epsilon$. There are also $1/\epsilon$ terms coming from the P_{ij}'s in Eq. (6). For example,

$$\tilde{t}P_{qg}(x)=-\frac{1}{\epsilon}\left[\frac{4\pi\mu^2}{Q^2}\right]^{\epsilon}\frac{\Gamma(1-\epsilon)}{\Gamma(1-2\epsilon)}\frac{x^2+(1-x)^2}{2}\ .$$

These $1/\epsilon$ terms all cancel, leaving a finite result for the nonleading correction terms K_1 and K_2.[8]

A comment is in order concerning the one-loop graphs shown in Fig. 4. The interference terms containing these graphs and the lowest-order Compton graphs also contribute to K_1 and have been included implicitly in the $2\rightarrow 3$ cross section appearing in Eqs. (2), (5), and (6). These virtual corrections have contributions proportional to $1/\epsilon^2$, $1/\epsilon$, and 1. The $1/\epsilon^2$ parts cancel against similar terms coming from the real-gluon-emission graphs. The $1/\epsilon$ parts cancel as discussed above. The final results for K_1 and K_2 are therefore finite.

We are interested in the corrections to the Compton subprocess coming from K_1 and K_2 so our final result takes the form

$$E\frac{d^3\sigma}{dp^3}(\gamma p\rightarrow\gamma+X)=\int dx_b\sum_{i=1}^{2f}G_{q_i/p}(x_b,Q^2)\left[E\frac{d^3\sigma}{dp^3}(\gamma q_i\rightarrow\gamma q_i)+K_1\right]+\int dx_b G_{g/p}(x_b,Q^2)K_2\ . \quad (7)$$

Two features of Eq. (7) are important. First, the Q^2-dependent distribution functions include next-to-leading order corrections. Second, α_s has been calculated to two-loop accuracy wherever it occurs in the functions appearing in Eq. (7).

In order to determine the various distribution functions required for this calculation we have used measurements of deep-inelastic electron, muon, and neutrino scatterings. A program which integrates the Altarelli-Parisi equations was used to fit data in the range $Q^2>10$ GeV^2 and $x<0.7$. These ranges were chosen to minimize possible effects of target-mass corrections and higher-twist terms. Fits were done using the leading-order (LO) terms and also including the next-to-leading-order corrections. The values of Λ obtained were $\Lambda_{\rm LO}=380$ MeV and $\Lambda_{\overline{\rm MS}}=440$ MeV, respectively ($\overline{\rm MS}$ refers to the modified minimal-subtraction scheme). The full results of this analysis will be reported elsewhere.[9]

The convention which we have adopted in this analysis is to use universal, process-independent parton distributions and to include the various next-to-leading-order corrections in the expressions for the relevant hard-scattering cross sections. The conventions used for the various coefficient functions are those of Ref. 10. This brings up a technical point concerning the calculation of the corrections term K_2 coming from the subprocess $\gamma g\rightarrow\gamma q\bar{q}$. The convention used for the deep-inelastic gluon coefficient function in Ref. 10 corresponds to not performing a spin sum on the initial gluon. From a practical standpoint, however, it is more convenient to do this spin sum when calculating the cross section for $\gamma g\rightarrow\gamma q\bar{q}$. Therefore, the gluon convention used in calculating K_2 does not match that used for determining nonleading corrections in deep-inelastic scattering. From a practical standpoint this has little impact on our final results. To change the coefficient function of the gluon in deep-inelastic scattering is very easy,[11] as it amounts to multiplying by $(1-\epsilon)$ before removing the $1/\epsilon$ part. The net effect of this change is to decrease the negative nonleading gluon correc-

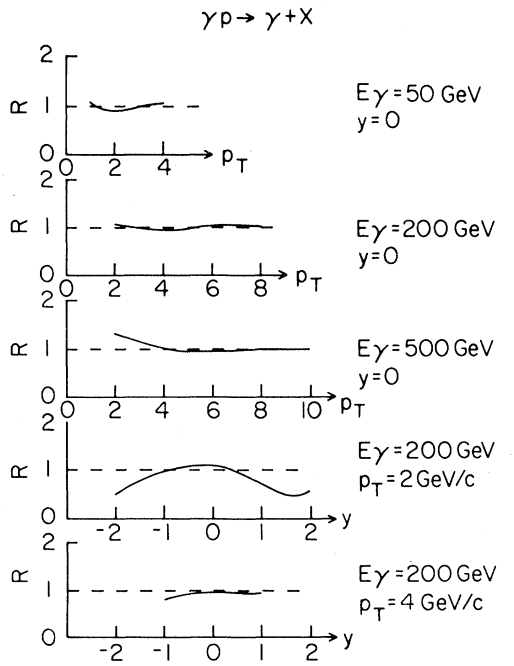

FIG. 5. The ratio R of the order-α^2 plus order-$\alpha^2\alpha_s$ calculation, Eq. (7), to the leading-logarithm Compton term.

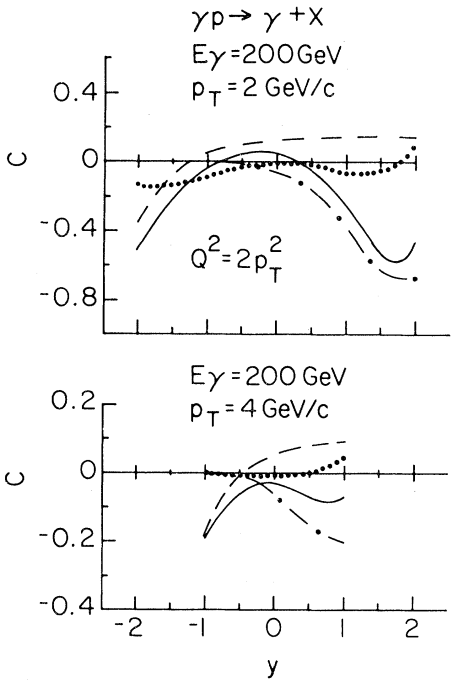

FIG. 6. The net correction $C=R-1$ from Fig. 5 versus y for two values of p_T. $Q^2=2p_T^2$ has been used. The full correction (solid lines) receives contributions from K_1 (dotted lines), K_2 (dashed-dot lines), and the distribution functions (dashed lines).

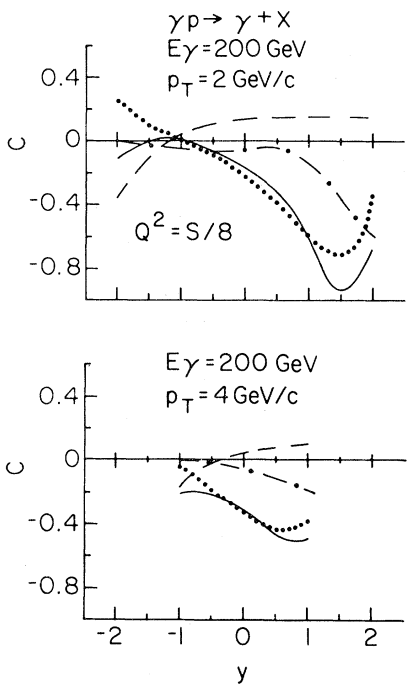

FIG. 7. The same as Fig. 6 except $Q^2=s/8$ has been used.

tion to F_2. This, in turn, is compensated by a small decrease in the size of the sea term which, through the momentum sum rule, leads to an increase of a few percent in the momentum fraction carried by the gluon. Of course, there are also some changes in the two-loop singlet anomalous dimensions[12,13] but they do not give a large effect. Thus, if we changed the deep-inelastic convention to match that used for K_2 we would find only a small change in the gluon distribution. However, the gluon distribution is still rather poorly known[14] and this uncertainty dominates that due to the convention adopted here. At any rate, we shall show below that K_2 is small over a significant fraction of phase space.

Our results for the overall order-$\alpha^2\alpha_s$ corrections are shown in Figs. 5–7. $Q^2=2p_T^2$ has been used here; the dependence on this choice will be discussed below. In Fig. 5 the results are shown in terms of R, defined as the ratio of the terms of order α^2 and $\alpha^2\alpha_s$ to the leading-logarithm Compton term alone. The leading-logarithm terms involving photon distribution and fragmentation functions have not been included. The kinematic regions chosen match those shown in Figs. 1–3. It is clear that in the region near $y=0$, $p_T>2$ GeV/c the corrections are very small. It is also in this region that the Compton process dominates over the other leading-logarithm backgrounds. Notice however, that for very forward values of rapidity and at relatively low p_T there is a region where the corrections become large. In order to understand this behavior it is useful to break the correction up into its component parts.

In Fig. 6 two examples are shown of the structure of the net correction $C=R-1$ as a function of y at fixed p_T. K_1 is negative and small while K_2 is negative and decreases rapidly with increasing p_T and increases with increasing y. The third contribution is due to the nonleading corrections to the distribution functions. This term changes sign for the two examples shown. For $p_T=2$ GeV/c it is clear that the large correction at forward y is due to K_2. In this region the range of values of x_b covered in Eq. (7) extends down close to zero:

$$x_{b\min}=p_T e^{-y}/(s-p_T e^{y}) .$$

The gluon distribution is large in this region, thereby giving rise to a large contribution from K_2. When a perturbative correction becomes this large it is clear that the result cannot be trusted. Furthermore, there are certainly other dynamical mechanisms which can also make significant contributions in this kinematic region. For example, it has

been shown in Ref. 15, using the results of Ref. 16, that the $\gamma g \to \gamma g$ scattering subprocess makes a non-neglible contribution for large y and small p_T. Therefore, in the region of large positive y one must go to the somewhat higher p_T values where the gluon correction becomes smaller (see Fig. 5).

In calculating the above results we have chosen the argument of α_s to be the same as that used for the distribution functions, i.e., $Q^2=2p_T{}^2$. In principle these two quantities can be different. However, to the order that we have calculated here, there are no strong coupling-constant-renormalization terms. Therefore, there is no rationale for choosing a different scale for α_s and the distribution functions. We also have the freedom to vary our choice of Q^2 in order to minimize the resulting corrections. It is difficult to choose an optimum value for Q^2, however, since there are three contributions to the overall correction and each one has a different kinematic structure. The choice used here gives small corrections everywhere except for large y and small p_T. We show in Fig. 7 the structure of the correction terms if we use the choice $Q^2=s/8$. It has been noticed previously[17] that this choice of factorization scale minimizes the corrections to large-p_T quark-quark scattering calculated in Refs. 5 and 17. It is clear from Fig. 7, however, that this choice gives very large correction terms to photon-quark scattering. We can conclude that these is no obvious universal choice of factorization scale Q^2 which will minimize the higher-order corrections for all large-p_T subprocesses simultaneously. It is clear then that there is a need for explicit calculation of each case.

V. CONCLUSIONS

In the large-transverse-momentum region inclusive photon photoproduction is dominated by the Compton subprocess. We have demonstrated that in the leading-logarithm approximation the contributions from subprocesses involving photon fragmentation and distribution functions decrease in importance rapidly with increasing p_T. We have also presented results for the order-$\alpha^2\alpha_s$ corrections coming from the $\gamma g \to \gamma q\bar{q}$ and $\gamma q \to \gamma qg$ subprocesses. These corrections were found to be very small for $p_T > 2$ GeV/c and rapidity values away from the forward region. For very forward rapidity values, the gluon correction K_2 becomes large and somewhat higher p_T values must be reached before the corrections are small again.

The small magnitude of the higher-order corrections means that the simple structure predicted by the Compton subprocess should appear in the high-p_T region. This reaction provides an example where the perturbation series appears to be rapidly converging. As a result, a precise measurement at high-p_T of this cross section should provide a useful test of the QCD-based description of large-momentum-transfer scattering.

ACKNOWLEDGMENTS

The authors wish to thank I. Hinchliffe for a useful discussion and correspondence. This work was supported in part by the U.S. Department of Energy.

APPENDIX A

In this appendix we summarize some expressions which are used in the leading-logarithm analysis. For a two-body reaction the invariant cross section and $d\sigma/dt$ are related by

$$E\frac{d^3\sigma}{dp^3}=\frac{s}{\pi}\frac{d\sigma}{dt}\delta(s+t+u)\,. \tag{A1}$$

The Compton-subprocess cross section is given by

$$\frac{d\sigma}{dt}=-\frac{2\pi\alpha^2 e_i{}^4}{s^2}\left[\frac{s}{u}+\frac{u}{s}\right]. \tag{A2}$$

The relevant order-$\alpha\alpha_s$ cross sections are

$$\gamma g \to q_i\bar{q}_i:\frac{d\sigma}{dt}=\frac{\pi\alpha\alpha_s e_i{}^2}{s^2}\left[\frac{u}{t}+\frac{t}{u}\right],$$

$$\gamma q_i \to q_i g:\frac{d\sigma}{dt}=-\frac{8\pi\alpha\alpha_s e_i{}^2}{(3s^2)}\left[\frac{t}{s}+\frac{s}{t}\right].$$

The expressions for the corresponding time-reversed reactions can be obtained by multiplying by color factors of $\frac{8}{9}$ and $\frac{1}{8}$, respectively. Expressions for the order-$\alpha_s{}^2$ subprocesses can be found in Ref. 18.

In carrying out the calculations in Sec. II it was useful to have simple parametrizations of the leading-logarithm photon distribution and fragmentation functions. The following expressions were used:

$$xGq_{i/\gamma}(x,Q^2)=F\left[e_i{}^2(1.81-1.67x+2.16x^2)\frac{x^{0.70}}{1-0.4\ln(1-x)}+0.0038(1-x)^{1.82}x^{-1.18}\right],$$

$$xG_{g/\gamma}(x,Q^2)=0.194F(1-x)^{1.03}x^{-0.97},$$

$$xD_{\gamma/q_i}(x,Q^2)=F\left[\frac{e_i^2(2.21-1.28x+1.29x^2)x^{0.49}}{1-1.63\ln(1-x)}+0.0020(1-x)^{2.0}x^{-1.54}\right],$$

$$xD_{\gamma/g}(x,Q^2)=xD_{g/\gamma}(x,Q^2),$$

where $F=(\alpha/2\pi)\ln(Q^2/\Lambda^2)$.

APPENDIX B

All of the calculational techniques used in this paper follow closely the methods of Ref. 5. First we discuss the calculation of the $2\rightarrow 3$ process $p_1+p_2\rightarrow k_1+k_2+k_3$ (the real bremsstrahlung graphs). The invariant, totally massless, three-particle phase space in $n=4-2\epsilon$ dimensions is

$$PS_3^{(n)}=\int\frac{d^{n-1}k_1}{(2\pi)^{n-1}2k_{10}}\frac{d^{n-1}k_2}{(2\pi)^{n-1}2k_{20}}\frac{d^{n-1}k_3}{(2\pi)^{n-1}2k_{30}}(2\pi)^n\delta^{(n)}(p_1+p_2-k_1-k_2-k_3),$$

$$=\frac{s}{(4\pi)^4\Gamma(1-2\epsilon)}\left[\frac{4\pi}{s}\right]^{2\epsilon}\int_0^1\int_0^1 v\,dv\,dw[v^2(1-v)w(1-w)]^{-\epsilon}\int_0^\pi d\theta_1\sin^{1-2\epsilon}\theta_1\int_0^\pi d\theta_2\sin^{-2\epsilon}\theta_2,$$

where we have expressed the final answer in the rest frame of k_2+k_3, i.e.,

$$k_2=k_{20}(1,\ldots,\sin\theta_1\sin\theta_2,\sin\theta_1\cos\theta_2,\cos\theta_1),$$

$$k_3=k_{30}(1,\ldots,-\sin\theta_1\sin\theta_2,-\sin\theta_1\cos\theta_2,-\cos\theta_1).$$

It is useful to define a set of invariants as follows:

$$s=2p_1\cdot p_2,$$

$$s_{ij}=2k_i\cdot k_j,$$

$$t_i=-2p_1\cdot k_i,$$

$$u_i=-2p_2\cdot k_i,\quad i,j=1,2,3.$$

So we have, letting k_1 correspond to the observed particle,

$$t_1=-s(1-v),$$

$$u_1=-svw,$$

$$s_{23}=sv(1-w).$$

Furthermore, we have in the k_2+k_3 rest frame

$$p_{10}=\frac{sv}{2s_{23}},$$

$$p_{20}=\frac{s(1-vw)}{2s_{23}},$$

$$k_{10}=\frac{s(1-v+vw)}{2s_{23}}.$$

Also, defining the angles ψ,ψ',ψ'' according to

$$t_1=-2p_{10}k_{10}(1-\cos\psi),$$

$$u_1=-2p_{20}k_{10}(1-\cos\psi'),$$

and

$$s=+2p_{10}p_{20}(1-\cos\psi''),$$

we have the useful relations

$$\sin^2\frac{\psi}{2}=\frac{(1-v)(1-w)}{1-v+vw},$$

$$\sin^2\frac{\psi'}{2}=\frac{v^2w(1-w)}{(1-vw)(1-v+vw)},$$

$$\sin^2\frac{\psi''}{2}=\frac{1-w}{1-vw},$$

from which expressions for $\cos^2\psi/2$, $\cos\psi$, etc., are easily obtained.

After squaring the matrix element, we are left with several hundred terms to integrate with respect to θ_1 and θ_2. Each term consists of at most four dot products in the numerator and denominator, e.g.,

$$\frac{st_1t_3}{u_3t_2u_2}.$$

Using

$$s+u_1+u_2+u_3=s+t_1+t_2+t_3=0$$

and partial fractioning gives for this term

$$\frac{st_1(s+t_1)}{(s+u_1)}\left[\frac{1}{t_2u_2}+\frac{1}{t_2u_3}\right]+\frac{st_1}{s+u_1}\left[\frac{1}{u_2}+\frac{1}{u_3}\right].$$

It is remarkable that in all known cases of totally massless $2\rightarrow 3$ scattering there are never any individual dot products of higher than the first power in the denominators,[19] even in n dimensions. The integrals with only one dot product (involving k_2 or k_3) in the denominator are straightforward, e.g.,

$$\int_0^\pi d\theta_1 \sin^{1-2\epsilon}\theta_1 \int_0^\pi d\theta_2 \sin^{-2\epsilon}\theta_2 \frac{1}{u_2} = \frac{1}{2p_{20}k_{20}}\frac{\pi}{\epsilon},$$

while integrals of the form

$$\int d\Omega_{23}^{(n)}\frac{1}{t_2u_3}=\frac{-1}{4p_{10}p_{20}{k_{20}}^2}\frac{\pi}{\epsilon}\left[\cos^2\frac{\psi''}{2}\right]^{-1-\epsilon} \times {}_2F_1\left[-\epsilon,-\epsilon,1-\epsilon;\sin^2\frac{\psi''}{2}\right],$$

are given in Ref. 5. The bulk of the calculation consists, therefore, of only rather mechanical repetition of these kinds of manipulations, and in fact we used the program SCHOONSCHIP[20] to handle all of the algebra of this calculation.

Concerning the virtual graphs, the calculation is by now rather standard. The only potential difficulty is in the evaluation of the box graph, i.e., one wants

$$I_4=\int\frac{d^nk}{(2\pi)^n}\times\frac{1}{k^2(k-k_1)^2(k-p_1)^2(k-p_1-p_2)^2}.$$

An easy way to proceed is to combine the last two propagators first,

$$\frac{1}{(k-p_1)^2(k-p_1-p_2)^2}=\int_0^1 dx\frac{1}{(k-p_1-xp_2)^4}.$$

Then the k integration is easy, and the remaining x integral is also straightforward, so we find

$$I_4=\frac{-i\Gamma(1+\epsilon)B(-\epsilon,-\epsilon)}{(-s)^{2+\epsilon}(4\pi)^{2-\epsilon}(1-v)}\left[\frac{-2}{\epsilon}\right]\times\left[-\frac{2}{\epsilon}+\ln(1-v)+\epsilon\frac{\pi^2}{2}\right],$$

where $s=2p_1\cdot p_2$, $t=-2p_1\cdot k_1$, $v=1+t/s$. A somewhat more elegant derivation of I_4 is given in Ref. 21.

[1] J. D. Bjorken and E. A. Paschos, Phys. Rev. 185, 1975 (1969).

[2] R. K. Ellis, H. Georgi, M. Machacek, H. D. Politzer, and G. G. Ross, Nucl. Phys. B152, 285 (1979); D. Amati, R. Petronzio, and G. Veneziano, *ibid.* B146, 29 (1978); A. H. Mueller, Phys. Rev. D 18, 3705 (1978).

[3] E. Witten, Nucl. Phys. B120, 189 (1977); C. H. Llewellyn Smith, Phys. Lett. 79B, 83 (1978).

[4] Tu Tung-sheng and Wu Chi-min, Nucl. Phys. B156, 493 (1979).

[5] R. K. Ellis, M. A. Furman, H. E. Haber, and I. Hinchliffe, Nucl. Phys. B173, 397 (1980).

[6] G. Altarelli and G. Parisi, Nucl. Phys. B126, 298 (1977).

[7] W. J. Marciano, Phys. Rev. D 12, 3861 (1975).

[8] The final answers for K_1 and K_2 contain 282 and 164 terms, respectively, and are not at all illuminating. The actual expressions are available from the authors upon request.

[9] A. Devoto, D. W. Duke, J. F. Owens, and R. G. Roberts, Florida State University Report No. FSU-HEP-820704 (unpublished).

[10] W. A. Bardeen, A. J. Buras, D. W. Duke, and T. Muta, Phys. Rev. D 18, 3998 (1978).

[11] G. Altarelli, R. K. Ellis, and G. Martinelli, Nucl. Phys. B157, 461 (1979).

[12] E. G. Floratos, D. A. Ross, and C. T. Sachrajda, Nucl. Phys. B152, 493 (1979).

[13] M. Gluck and E. Reya, Phys. Rev. D 25, 1211 (1982).

[14] D. W. Duke, J. F. Owens, and R. G. Roberts, Nucl. Phys. B195, 285 (1982); H. Abramowicz *et al.*, Z. Phys. C 12, 289 (1982).

[15] M. Fontannaz and D. Schiff, Orsay Report No. LPTHE82/7 (unpublished).

[16] B. L. Combridge, Nucl. Phys. B174, 243 (1980).

[17] W. Furmanski and W. Slominski, Jagellonian University Report No. TPJU-11/81 (unpublished).

[18] J. F. Owens, E. Reya, and M. Gluck, Phys. Rev. D 18, 1501 (1978).

[19] F. A. Berends, R. Kleiss, P. de Causmaecker, R. Gastmans, and T. T. Wu, Phys. Lett. 103B, 124 (1981).

[20] H. Strubbe, Comput. Phys. Commun. 8, 1 (1974).

[21] S. Papadopoulos, A. P. Contogouris, and J. Ralston, Phys. Rev. D 25, 2218 (1982).